Automatic recognition of a piping system from laser scanned points by eigenvalue analysis

Kazuaki Kawashima[1,a], Satoshi Kanai[1,b] and Hiroaki Date[1,c]

[1]Graduate School of Information Science and Technology, Hokkaido University,

Sapporo 060-0814, Japan

[a]k_kawashima@sdm.ssi.ist.hokudai.ac.jp, [b,c](kanai, hdate)@ssi.ist.hokudai.ac.jp,

Keywords: Laser scanning, Point clouds, As-built model, Piping system, Reverse engineering

Abstract. In recent years, changes in plant equipment have been becoming more frequent, and as-built modeling of plants from large-scale laser scanned data is expected to make their rebuilding processes more efficient. The purpose of our research was to propose an algorithm which can automatically recognize piping systems from massive terrestrial laser scanned point clouds of plants. Point clouds of a piping system can be extracted based on eigenvalue analysis and using region-growing from the laser scanned points. Eigenvalue analysis of the point clouds and point normals then allows for the recognition of straight portions of pipes. Connecting parts can also be recognized from the connection relationship between pipe axes and their neighboring scanned point distributions.

1. Introduction

In recent years, as-built modeling of existing plants from laser scanned point clouds is expected to avoid unintended works and make the plant rebuilding process more efficient. However, the laser scanned data of existing plants has a huge number of points, and includes a large amount of noise. Therefore, recognizing each engineering object from these enormous and noisy point clouds and building 3D models of the plants are nearly impossible or very time consuming when doing it in a manual way. Thus, automating as-built model construction from the point clouds needs to be strongly encouraged in plant engineering.

Plants consist of many types of objects. Among them, piping systems are especially important and are renovated frequently. Thus, the purpose of our research was to propose a new algorithm that can automatically recognize piping systems from a massive laser scanned point cloud of a plant. A piping system consists of various piping elements and connection relationships; straight pipes, connecting parts, such as T-junctions and elbows, indicators, valves, etc. Also, the connection relationship defines the logical connectivity between these piping elements.

So far, several research studies have been done to recognize a piping system from laser scanned data of plant equipment. Masuda et al proposed an algorithm which can recognize planes and cylinders from a single scan data of plants[1]. However, a region to be recognized has to be selected manually in advance. Moreover, a number of algorithms have also proposed which reconstruct a 3D model from the combination of a point cloud and other types of data such as photos[2], or priori CAD models[3]. However, the recognition algorithms of the piping system require supplementary data other than a point cloud, such as plant photos or prespecified geometric primitives. Johnson also proposed an algorithm which can semi-automatically build a 3D model by matching a point cloud to a CAD model using spin images[4]. However, this also requires preparation for the recognition of 3D objects in advance.

Thus, existing researches can not recognize pipes in a fully automatic way, and can not be directly applied to a registered point cloud, and require geometric models of recognition objects. Therefore, we propose a new algorithm that can fully-automatically recognize piping elements and their connection relationships from a registered laser scanned point cloud of a plant.

2. Algorithm Overview

As shown in Fig.1, our algorithm consists of three steps. In the first step (A1), points on background objects, such as floors and walls, are extracted and removed from the whole scanned point cloud of a plant. Then, in the second step (A2), points on straight pipes, here after referred to "pipe points," are extracted from the remaining points, and their radii and the positions of the pipes are recognized. Also, axis segments of the pipes are calculated. Then, in the third step (A3), the connection relationships among the extracted straight pipes are recognized using the positions of the axis segments and their neighboring scanned point distributions. The detailed processes of steps (A1), (A2) and (A3) are shown in sections 3, 4 and 5, respectively.

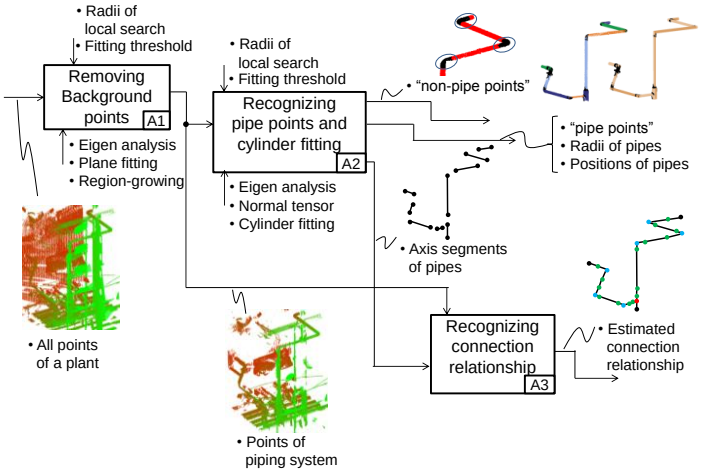

Fig.1 Top-level process of piping system recognition

3. Removing Background points

In order to estimate the local geometric property in the neighborhood of a point i, first, the covariance matrix M_i is calculated for a set of points $N(i,r_1)$, where $N(i,r_1)$ is a set of neighboring vertices contained in the sphere of the radius r_1 centred at i. Then, the eigenvalues $\lambda_1,\lambda_2,\lambda_3$ $(\lambda_1 \geq \lambda_2 \geq \lambda_3 \geq 0)$ and corresponding eigenvectors $\mathbf{e}_1,\mathbf{e}_2,\mathbf{e}_3$ are obtained. Finally, the feature quantities S_1,S_2,S_3 of the local geometry of neighboring points[5] are calculated by equation (1).

$$S_1 = \lambda_1 - \lambda_2, \quad S_2 = \lambda_2 - \lambda_3, \quad S_3 = \lambda_3 \tag{1}$$

Then, a seed point s on a plane which satisfies $S_2 = \max(S_1,S_2,S_3)$ and has maximum value of S_2 for all points is selected. Then, a plane P is fitted to the neighboring points $N(s,r_2)$ using LMedS[6]. If the average of distances between P and $N(s,r_2)$ is more than τ_p, $N(s,r_2)$ would exist on curved surfaces such as pipes, and $N(s,r_2)$ could be classified as "non-planar points". Otherwise, $N(s,r_2)$ are classified as "planar points." Then, points which fit to plane P are extracted by applying the region growing method. First, neighboring points $N(s,r_3)$ are added to a region. Then, a plane P is fitted to the new added points by LMedS. If the average distance between P and the new added points is less than τ_p, each of the points are then chosen as a new seed point. The above steps are iterated until unclassified points still exist in neighborhoods of the new seed points or until the average distance is more than τ_p. Finally, in the region, the points which fit to plane P are classified into "planar points." The plane extraction process is repeated until all points are classified. At last, the extracted "planar points" are not used for the piping system recognition and are removed.

4. Recognizing points on pipes and cylinder fitting to pipes

In this section, the detailed process of the recognizing points on pipes and cylinder fitting to pipes for "non-planar points" are described. The detailed flow of the process is shown in Fig.2.

4.1. Estimating normal vectors

First, the covariance matrix M_i is calculated for a set of points $N(i,r_4)$. Then, the eigenvalues $\lambda_1,\lambda_2,\lambda_3$ and corresponding eigenvectors $\mathbf{e}_1,\mathbf{e}_2,\mathbf{e}_3$ are obtained similar to as in Section 3. If we set r_4 to smaller than the radius of pipe R, the vector $\mathbf{e}_3$ will approximate the normal at i. Thus, $\mathbf{e}_3$ is determined to be the initial normal vector $\mathbf{n}_i'$ at point i. Finally, the normal vector $\mathbf{n}_i$ at vertex i is calculated by a quadratic polynomial surface fitting[7] to a set of points $N(i,r_4)$.

4.2. Extracting points on pipes

First, a normal tensor T_i at point i [8] is calculated by equation (2) for a set of points $N(i,r_5)$.

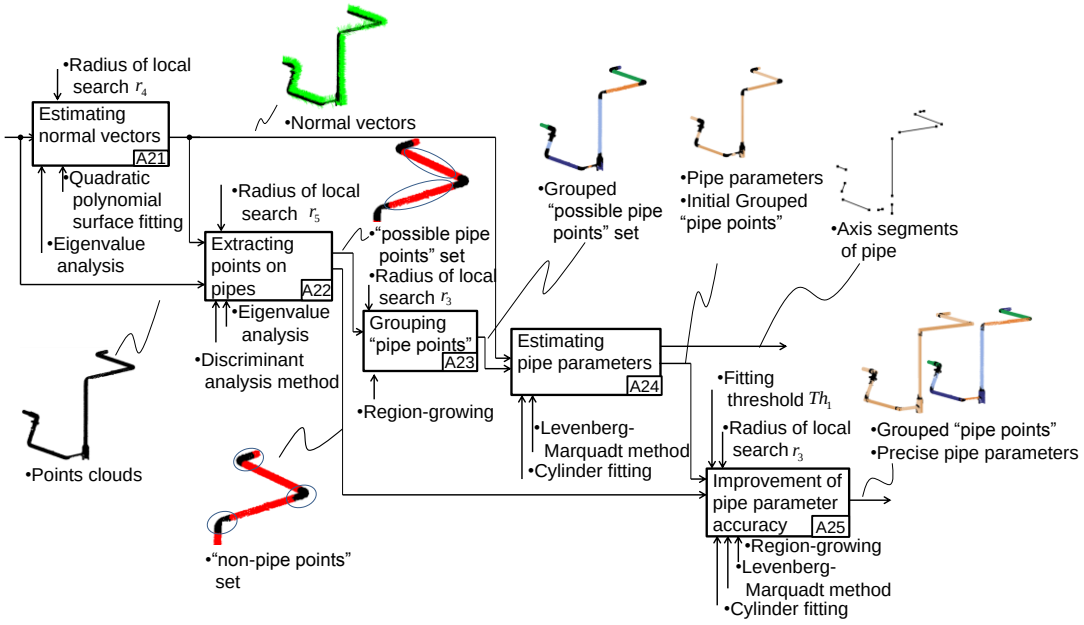

Fig.2 The detailed process of recognizing points on pipes and model fitting to the pipes

$$T_i = \frac{1}{|N(i,r_5)|}\sum_{j\in N(i,r_5)} \mathbf{n}_j{}^T \cdot \mathbf{n}_j \qquad (2)$$

Then, the eigenvalues $\hat{\lambda}_1, \hat{\lambda}_2, \hat{\lambda}_3$ $(\hat{\lambda}_1 \geq \hat{\lambda}_2 \geq \hat{\lambda}_3 \geq 0)$ and corresponding eigenvectors $\mathbf{m}_1, \mathbf{m}_2, \mathbf{m}_3$ are obtained by eigenvalue analysis of T_i. These eigenvalues and eigenvectors show spatial distributions of the normal gauss image, as shown in Fig.3. For example, at a point i on a straight portion of pipe, the normal vectors in $N(i,r_5)$ exist almost on one plane. Then, $\hat{\lambda}_3$ becomes much smaller than $\hat{\lambda}_1$ and $\hat{\lambda}_2$. While at a point on an elbow or a T,Y junction, the normal vectors are distributed three-dimensionally. Then, $\hat{\lambda}_3$ becomes larger than that of the former case. Thus, limiting $\hat{\lambda}_3$ enables all scanned points to be classified into "possible pipe points" and "non-pipe points." The threshold value is determined by the discriminant analysis method [9].

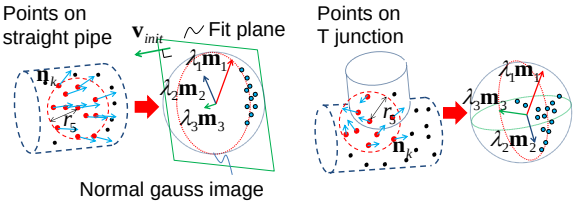

(a) "pipe point" (b) "non-pipe point"

Fig.3 Normal gauss image and eigenvectors of normal tensor

4.3. Grouping "possible pipe points"

Possible pipe points on one straight portion of a pipe are integrated into a single region by applying the region growing method. First, a seed point s of a region is chosen from the *possible pipe points* at random. Then, a set of neighbouring points $N(s,r_3)$ are added to a region. Each of these added points are then chosen as a new seed point, and other *possible pipe points* adjacent to each seed point are added to the region. The above process is repeated until *possible pipe points* exist in neighborhoods of the seed points.

4.4. Extracting initial pipe parameters

After grouping the *possible pipe points*, the axes of the pipes and their radii are estimated.

First, a normal gauss image is created from all *possible pipe points* in a region. Then, a plane is fitted to the gauss image using LMedS, and the normal vector of the plane is determined to be an initial axis vector $\mathbf{v}_{init}$. In the LMedS, the number of samplings is 100 in this paper. Then, all *possible pipe points* in the region are projected to the plane, and a circle is fitted to the projected points by the least-square method. As a result, the center point and the radius of the fitted circle respectively become an initial point on the axis $\mathbf{p}_{init}$ of the pipe, and an initial radius r_{init} of the pipe. Then, a cylinder is precisely fitted to the points of the region using the non-linear least square method [10].

Then, based on the obtained radii r and average distances $\bar{\varepsilon}$ between the fitted cylinder surface and points in a group, *possible pipe points* groups which satisfy $(\bar{\varepsilon} > \varepsilon_\tau) \vee (r < r_{\min}) \vee (r > r_{\max})$ are moved into *non-pipe points*.

Then, the remaining *possible pipe points* in the region are projected on to its cylinder axis, and two end points of the projected points are determined as edge points e, e'. The segment connecting e with e' is used for recognizing pipe connection relationships, as described in Section 5.

4.5. Correcting the pipe parameters

In the result of section 4.2, *non-pipe points* still include the straight portion of pipes due to the limitation of the discriminant analysis. To improve the fitting and recognition accuracy of pipes, the miss-classified points included in the *non-pipe points* are extracted from the set and are added to the *pipe point*, and cylinders are re-fit to the *pipe points*. In this step, a seed point s which exists nearest to a fitting cylinder is chosen from *non-pipe points*. Then, the *non-pipe points* within the distance τ_c from the cylinder are only selected from the points $N(s, r_3)$. The selected points are then added to the pipe region, and a cylinder is fitted once again. Then these selected points become new seed points. The above steps are repeated until a *non-pipe point* which lies within the distance τ_c from the fitted cylinder exists in the neighborhood of the new seed points.

5. Recognizing connection relationship

In order to recognize the straight portions of a pipe occluded by other pipes and to identify junctions among the pipes, the connection relationship between pipe regions is recognized by the relative positions and orientations of the axis segments created in Section 4.4.

An axis segment S_i of a pipe has a centre point p_i, two edge points e_i, e_i', outward unit axis vectors $\mathbf{u}_i, \mathbf{u}_i'$ and a radius of the fitted cylinder R_i. Based on the segments, occluded portions of pipes are interpolated, and T and Y junctions and elbows are identified progressively.

5.1. Recognition of occluded pipe portions

First, pairs of nearly collinear axis segments S_i and S_j which satisfy $|\mathbf{u}_i \cdot \mathbf{u}_j| > \tau_{inner}$ and $|\mathbf{u}_i \cdot \mathbf{p}_{ij}| > \tau_{inner}$ are selected. $\mathbf{p}_{ij}$ is a unit vector of a line connecting the two segment center points p_i and p_j. The threshold τ_{inner} was set to be 0.98 in our experiments.

Then, the segment pair whose endpoints e_i, e_j take the minimum distance is selected. If the distance is less than τ_l, a new pipe segment S_{new} is inserted between the endpoints e_i and e_j. A radius of segment S_{new} is inherited from S_i and S_j as an average of the radii R_i and R_j respectively.

5.2. Recognition of Connecting parts

After the interpolation of occluded straight pipe portions, junction parts which connect multiple pipes are identified. T,Y-junctions first, a pair of segments S_i, S_j which satisfy $|\mathbf{q}_j - \mathbf{q}_i| < \tau_{skew}$ and $|\mathbf{e}_i' - \mathbf{e}_i| > |\mathbf{q}_i - \mathbf{e}_i|$ are selected. $\mathbf{q}_i$ and $\mathbf{q}_j$ are position vectors of the intersection points of the common perpendicular line of two lines L_i and L_j which respectively pass through end points e_i and e_j and are collinear to axis segments S_i and S_j, and τ_{skew} is the threshold for the skew distance between L_i and L_j.

Then, if the segment pair gives the minimum distance $|\mathbf{e}_i - \mathbf{q}_j|$ and the distance is less than τ_l, the type of connecting part is classified by the following steps.

First, as shown in Fig.4(a), a sphere of radius ρ_s is placed centred at the intersection point q_j. Then, points near the sphere surface are selected. Then, the planes each of whose normal is equal to $\mathbf{u}_i$ or $\mathbf{u}_j$ are fitted to the selected points. Also, the points are projected to each fitted planes as shown in Fig.4(b). Then, a circle is fitted to each of the projected points using Hough transform, as shown in Fig.4(c). Then, the number of the connect fitting circles is counted whose radii ρ_i, ρ_j satisfy the range $r_{\min} < r < r_{\max}$. By iterating the above steps with different sphere radii ρ_s, the most frequent number of intersecting circles N_c is selected. If N_c satisfies $N_c = N_a$ where $N_c = 3$ (T,Y-junctions), $N_c = 2$ (elbows), a T,Y-junction or an elbow is determined to exist. If so, a new segment S_{new} is inserted so as to connect e_i and q_j. The radius of segment S_{new} is set to be identical to the radius R_i of the original segment S_i.

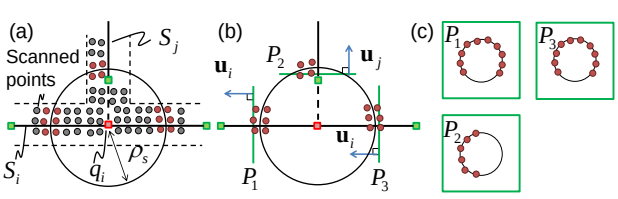

Fig.4 Connecting part recognition

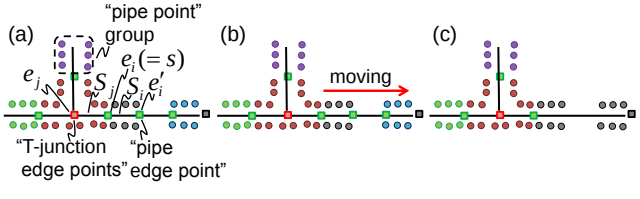

Fig.5 Integrating axis segments

5.3. Removing interfering segments

Pipes corresponding the inserted segments described in 5.1 and 5.2 are checked whether they collide with other objects, and interfering segments are removed. If the minimum distance l between an inserted segment and scanned point clouds is less than the threshold τ_l, the segment is removed.

5.4. Classification of connecting parts

After inserting the new segments between the existing pipe segments, each edge point e_i is finally classified into one of the five point types; "pipe edge point," "T-junction edge point," "Y-junction edge point," "elbow edge point," "reducer edge point." The classification is done on the basis of the number of connecting segments and the angle among the connecting segments.

5.5. Integrating axis segments on the same pipe

In order to obtain precise pipe region, the devided pipe regions on a pipe are integrated into one region based on the classified edge points.

First, an edge point e_i which satisfies one of the following conditions (1) and (2) is selected as a start point s as shown in Fig.5(a); (1) e_i is connected only one axis segment S_i, (2) (e_i is a *pipe edge point*), and (an edge point e_i' of axis segment S_i is a *pipe edge point*), and (another edge point e_j' of connecting another axis segment S_j is not a *pipe edge point*). Next, if the edge point e_i' on the other side of axis segment S_i which connects to the start point is a *pipe edge point*, the point cloud which corresponds to S_i is added to a region, and the start point is moved to edge point e_i', as shown in Fig.5(b). The above process is itelated while point e_i' is not a *pipe edge point* and a region of *pipe points* on one pipe are obtained as shown in Fig.5(c).

6. Results

As experiments of the recognition, as shown in Fig.6(a) and Fig.7(a), one large point cloud was scanned from a real oil rig by a laser scanner (Cyra Technologies CYRAX2500), and another cloud from an air-condition room by another laser scanner (Leica HDS6000). They had 4,524,324 points and 4,075,752 points, respectively. The thresholds of the oil rig recognition were $r_1 = 200.0$, $r_2 = 200.0$, $r_3 = 20.0$, $r_4 = 30.0$, $r_5 = 200.0$, $\tau_p = 10.0$, $\tau_c = 5.0$, $\tau_l = 1000.0$, $\tau_{skew} = 50.0$, $\bar{\varepsilon} = 10.0$, $r_{\max} = 100.0$, and $r_{\min} = 40.0$mm. Those of the air-congition room recognition were $r_1 = 200.0$, $r_2 = 200.0$, $r_3 = 20.0$, $r_4 = 30.0$, $r_5 = 200.0$, $\tau_p = 3.0$, $\tau_c = 5.0$, $\tau_l = 1000.0$, $\tau_{skew} = 50.0$, $\bar{\varepsilon} = 20.0$, $r_{\max} = 300.0$, $r_{\min} = 30.0$mm. The total recognition process took 6119 sec and 37873 sec, respectively, using a PC (Core-i7).

The final recognition results of cylinder fitting to the pipe portions and of the connection relationships are shown in Fig.6(b) and Fig.7(b), respectively. The recognition accuracies of the pipes and the connecting parts are also shown in Table.1 and Table.2, respectively. The recognition accuracies of the pipe are about 84%~85%. While, those of the connecting parts were still about 40% and 54%, respectively. The reason for this mis-classification was that pipes which connected between connecting parts were not correctly recognized, and a small number of flanged connecting parts could not be recognized in the step of the connecting parts recognition algorithm. This problem should be improved as our future work.

7. Conclusions

A new algorithm was proposed that can automatically recognize a piping system from scanned point clouds of a plant. The points of piping systems could be extracted by eigenvalue analysis. The points on straight pipes could be recognized by the normal tensor, and the radii and positions of pipe segments could be recognized by cylinder fitting using the non-linear least square method. The connecting relationship between pipes could be classified based on the relative positions and orientations of the fitted cylinders and their neighboring point distribution. The recognition was verified by large-scalescanned points of plants, and the results showed the potential effectiveness of the proposed algorithm.

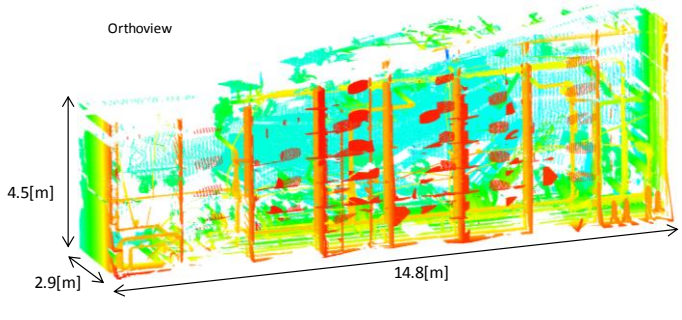

(a) Scanned point cloud

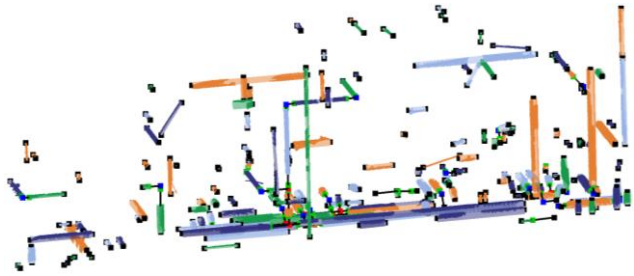

(b) Final recognition

Fig.6 Recognition results of piping system of oil rig

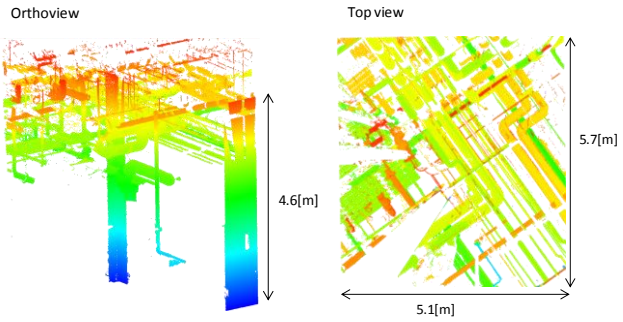

(a) Scanned point cloud

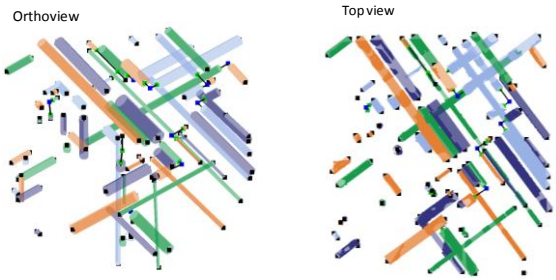

(b) Final recognition

Fig.7 Recognition results of piping system of air-condition room

Table.1 Accuracy of piping system recognition of oil rig

(a) Pipe

		Result of automatic recognition			
		Pipe	Other	Total	Recognition rate %
True Class	Pipe	92	17	109	84.4
	Other	37	174	211	-
	Total	129	191	320	-

(b) Connecting parts

		Result of automatic recognition							
		Elbow	T-junction	Y-junction	Others	Not recognized	Total	False Negative %	False Positive %
True Class	Elbow	22	1	0	0	28	51	56.8	3.9
	T-junction	0	7	0	0	6	13	46.1	7.7
	Y-junction	0	0	0	0	0	0	-	-
	Others	2	0	0	0	0	2	-	-
	Total	24	8	0	0	34	66		--

Table.2 Accuracy of piping system recognition of air-condition room

(a) Pipe

		Result of automatic recognition			
		Pipe	Other	Total	Recognition rate %
True Class	Pipe	35	6	41	85.3
	Other	20	58	78	-
	Total	55	64	119	-

(b) Connecting parts

		Result of automatic recognition							
		Elbow	T-junction	Y-junction	Others	Not recognized	Total	False Negative %	False Positive %
True Class	Elbow	6	0	0	0	9	15	60.0	20.0
	T-junction	0	0	0	0	1	1	0.0	0.0
	Y-junction	0	0	0	0	0	0	-	-
	Others	3	0	0	0	0	3	-	-
	Total	9	0	0	0	10	19		--

References

[1] H Masuda, Extraction of Surface Primitives using Geometric Constraints of Objects, In proceedings of JSPE Semestrial Meeting, vol.2009A, (2009) 899-900

[2] T. Rabbani, F. Heuvel, 3d Industrial Reconstruction by Fitting CSG Models to a Combination of Images and Pointclouds, ISPRS and Spatial Information Sciences, 35(B3), (2004) 7

[3] B. Aurelien, R Chaine, R Marc, G Thibault, S Akkouche, Reconstruction of Consistent 3D CAD Models from Point Cloud Data Using A Priori CAD Models, ISPRS Workshop Laser Scanning 2011, (2011) submission-26

[4] A. Johnson, R. Hoffman, J. Osborn, M. Hebert, A system for semi-automatic modeling of complex environments, Proc of IEEE International Conference on Recent Advances in 3-D Digital Imaging and Modeling, (1997) 213

[5] G. Medioni, C. Tang, M. Lee, Tensor Voting: Theory and Applications, Proc. 12eme Congres Francophone AFRIF-AFIA de Reconnaissance des Formes et Intelligence Artificielle, (2000)

[6] R. A.Maronna, R. D.Martin, V. J. Yohai: Robust Statistics: Theory and Methods, U.K., Wiley, (2006) 126.

[7] T Mizoguchi, H Date, A Kanai, T Kishinami, Quasi-optimal mesh segmentation via region growing/merging, In Proceedings of the ASME 2007 International Design Engineering Technical Conferences and Computers and Information in Engineering Conference, DETC 2007-35171, (2007) 547-556

[8] Q. Zhou, U. Neumann, Fast and Extensible Building Modeling from Airborne LiDAR Data, Proc of the 16th ACM SIGSPATIAL International Conference on Adcances in Geographic Information Systems (2008)

[9] W. Klecka, Discriminant analysis, SAGE, Sage university papers series, (1980)

[10] C. Shakarji et al, Least-Squares Fitting Algorithms of the NIST Algorithm Testing System, SAGE, Journal of Research of the National Institute of Standards and Technology, 103(6), (1998), 633